Microprocessors and Microsystems 000 (2016) 1–12

Contents lists available at ScienceDirect

Microprocessors and Microsystems

journal homepage: www.elsevier.com/locate/micpro

Methods for reliable estimation of pulse transit time and blood pressure variations using smartphone sensors

Alair Dias Junior[a,b,*], Srinivasan Murali[c], Francisco Rincon[a,c], David Atienza[a]

[a] Embedded Systems Laboratory (ESL), EPFL, Switzerland
[b] FUMEC University, Brazil
[c] SmartCardia GmbH, Switzerland

ARTICLE INFO

Article history:
Received 8 January 2016
Revised 20 April 2016
Accepted 1 June 2016
Available online xxx

Keywords:
Pulse transit time
Arterial blood pressure
Smartphone
Bio-medical signal processing

ABSTRACT

Hypertension is known to affect around one third of adults globally and early diagnosis is essential to reduce the effects of this affliction. Today's Blood Pressure (BP) monitoring cuffs are obtrusive and inconvenient for performing regular measurements, and continuous non-invasive blood pressure devices are too complex and expensive for ambulatory use. Hence, there is a strong need for affordable systems that can measure blood pressure (BP) variations throughout the day as this will allow to monitor, diagnose and follow-up not only patients at risk, but also healthy population in general for early diagnosis. A promising method for arterial BP estimation is to measure the Pulse Transit Time (PTT) and derive pressure values from it. However, current methods for measuring this surrogate marker of BP require complex sensing and analysis circuitry and the related medical devices are expensive and inconvenient for the user. In this paper, we present new methods to estimate PTT reliably and subsequently BP, from the baseline sensors of smartphones. This new approach involves determining PTT by simultaneously measuring the time the blood leaves the heart, by recording the heart sound using the standard microphone of the phone, and the time it reaches the finger, by measuring the pulse wave using the phone's camera. We present algorithms that can be executed directly on current smartphones to obtain clean and robust heart sound signals and to extract the pulse wave characteristics. We also present methods to ensure a synchronous capture of the waveforms, which is essential to obtain reliable PTT values with inexpensive sensors. Additionally, we combine Autocorrelation and Fast Fourier Transform (FFT)-based methods for reliably estimating the user heart rate (HR) from his/her heart sounds, and describe how to use the calculate HR to compensate for the camera frame rate variations and to improve the robustness of PTT estimation. Our experiments show that the computational overhead of the proposed processing methods is minimum, which allows real-time feedback to the user, and that the PTT values are fully accurate (beat-to-beat), thereby enabling state-of-the-art smartphones to be used as affordable medical devices.

1. Introduction and related work

With an ageing society and increasing prevalence of noncommunicable diseases, there is a strong need for systems that can provide quick and continuous healthcare of people. Cardiovascular diseases (CVDs) are the leading causes of disability and death in the world. According to a recent World Health Organization (WHO) report, 17.3 million people died from CVDs in 2008. A large percentage of the CVD can be prevented, but they continue to increase due to the lack of adequate screening and timely availability of diagnostic and preventive measures. More than 50% of CVD related deaths arise from complications of hypertension and 40% of adults aged 25 and above were diagnosed with hypertension worldwide in 2008 [1]. In this endemic scenario, prevention and early diagnosis are key to reduce the economic and social costs related to hypertension.

During the last decades, ambulatory measurement of arterial blood pressure (BP) has been prescribed to patients suspected to suffer from hypertension [2]. Current 24 h ambulatory blood pressure monitoring (ABPM) devices, nevertheless, are cumbersome equipments based on mechanical or oscillometric recordings and require a pressure cuff to be placed on the patient's upper arm or wrist. The periodic inflation of the cuff, usually every 20 min, is uncomfortable and noisy, disturbing the patient sleep and interfering with the BP measures themselves. Moreover, other continuous

* Corresponding author at. Rua Cobre 200 - Belo Horizonte, Brazil.
E-mail addresses: alair.djr@fumec.br, alair.junior@gmail.com (A. Dias Junior), srinivasan.murali@smartcardia.com (S. Murali), francisco.rincon@smartcardia.com (F. Rincon), david.atienza@epfl.ch (D. Atienza).

http://dx.doi.org/10.1016/j.micpro.2016.06.001
0141-9331/

non-invasive beat-to-beat BP monitoring devices [3] are too complex and expensive, and thus not convenient for ambulatory monitoring. It is, therefore, clear that there is a strong need for new Non-Invasive Blood Pressure (NIBP) measuring methods that are able to track BP variations throughout the day, in order to monitor, diagnose and follow-up patients at risk, as well as for healthy people for early diagnosis.

Several recent works have presented novel ways of measuring BP using different sensors [2–9]. The most promising ones measure the pulse transit time (PTT) differences between different waveforms, such as the electrocardiogram (ECG), photo-plethysmogram (PPG), phonocardiogram (PCG), impedance cardiogram (ICG), electrical impedance tomography (EIT) or a combination of them.

The underlying principle of the PTT-based approach is that arterial stiffness increases with BP in a predictable manner, also affecting the pulse wave velocity (PWV) along the arterial tree. Hence, by measuring the time the pulse wave takes to travel from one point of the arterial tree to another, it is possible to calculate the PWV and estimate BP using elasticity-based models of the blood vessels.

The use of PTT to derive BP variations has been explored over the last decades. For example, the Casio BP-100 [10] was a pioneering consumer watch that could measure pulse and ECG (by touching the watch from the other hand) and derive the PTT-based BP variations. A more recent approach is presented in [2] where a chest sensor is proposed to assess PTT using ECG, PPG, and ICG. By acquiring all signals on the chest, the PTT is computed over the elastic arteries and, according to the authors, this results in more accurate PTT measurements.

Recent research has shown that reliable BP measurements with PTT-based methods require, at least, an initial calibration to model the individual PTTxBP relationship [4], or even a periodic calibration process to compensate for intra-patient variations, specially due to the vasomotion phenomenon. Hence, a standard BP measurement device based on mechanical or oscillometric recordings is used during the calibration step to feed the model with the required parameters. In particular, [3] details a system to estimate BP at the femoral artery using an ECG and a PPG sensor placed on the patient's thumb to calculate PTT. The system includes a brachial pressure cuff to perform periodic calibrations (every 4-8 hours) to compensate for inter and intra-patient variations of the PTTxBP relationship, which shows the feasibility of meeting U.S. Food and Drug Administration (FDA) standards for medical grade devices using PTT-based methods.

Additional research on the calibration step using different points of the patient body is presented in [8], where a BP monitor consisting of twin in-line PPG sensors that measure the pulse arrival time (PAT) using the wrist and little finger is described. The PTT is calculated by subtracting one PAT from another. The calibration procedure is performed by a set of wrist movements that changes the external pressure applied by a band placed on the patient's wrist, but the results do not assess the precision of the calibration procedure. Similarly, [11] proposes the use of hydrostatic pressure changes, but no consistent experimental results have validated this approach so far.

Beyond the concern on calibration methodologies for PTT, the reality is that a large set of works have evaluated the use of PTT as a surrogate marker for BP. We refer the interested reader to Henning and Patzak [12], which provide a complete summary of most of the relevant works, and come to the conclusion that PTT is suitable for continuous monitoring of BP. The authors state that previous works results are encouraging enough for further clinical evaluation of PTT-based BP measurement methods.

The major challenge of using PTT to estimate BP, nevertheless, is the high degree of exactness and precision required in the acquisition and delineation steps. Usually, this is achieved by using expensive high-precision sensors and heavy signal processing techniques. However, to deliver an ambulatory solution for continuous NIBP measurements, low cost and ease of use are key factors.

A work that is more in line with these restrictions uses smartphones to measure PTT and estimate differential blood pressure using two different setups [5]. The first one uses two smartphones synchronized via a self-designed bluetooth synchronization protocol. One device records the PPG using the camera while the other is used to record the sounds from the heart. Due to this synchronization procedure, the smartphones must be rooted (i.e., user applications needs to be given permission to run privileged commands), replacing their stock configuration. The second setup uses one smartphone and a customized external microphone to record heart sounds, which outlines the capabilities of smartphones for PTT measurements. However, methods are still missing to perform robust and reliable PTT measurement using the baseline sensors of smartphones with stock configuration.

The use of smartphones for health applications is rapidly increasing [13], mainly due to the high penetration of this technology, which is becoming a very powerful tool to bring healthcare to remote and rural areas, specially in developing countries. Although the widespread adoption of smartphones to track health is still a challenge, many recent studies have proven that they can help to track and improve different conditions, such as type 1 diabetes [14], Parkinson's disease [15], etc.

In this work we describe new on-board robust methods to obtain clean heart sound signals and to extract the pulse wave characteristics using just baseline sensors of smartphones with stock configuration. We also present methods to ensure a synchronous capture of the waveforms, which is essential to obtain reliable PTT values with inexpensive sensors. We combine Autocorrelation and Fast Fourier Transform (FFT)-based methods for reliably estimating the user heart rate (HR) from his/her heart sounds, and describe how to use the calculated HR to compensate for the camera frame rate variations and to improve the robustness of PTT estimation.

The rest of the paper is structured as follows. In Section 2 we present the overview of the proposed solution and how all the subsystems work together. Then, Section 3 describes in detail the signal acquisition and processing steps for both PPG and PCG recordings. Some of the theories and experiments described in this paper were first presented in [16], Section 4, nevertheless, the current paper presents further improvements on the method, describing how the heart rate can be calculated from the heart sounds and how it can be used to improve the user experience and the accuracy of the method. Experimental results are presented next, in Section 5, followed by the discussions and conclusions in Sections 6 and 7.

2. Background and method overview

PTT calculation involves the acquisition of the pulse arrival time (PAT) at two different points of the arterial tree. Once the PATs are computed, the PTT can be calculated by the formula presented in Eq. (1).

$$PTT = PAT_1 - PAT_0 \tag{1}$$

The first point on the arterial tree, which corresponds to PAT_0, is usually called proximal point, and the point used to determine PAT_1 is called distal point. The method we describe in this section uses the smartphone's internal microphone and camera to reliably compute the PATs at the proximal and distal points, respectively, and then calculate the PTT.

Differently from most of the previous works, here PAT_0 is computed from the heart sounds instead of the R-peak of the ECG wave. During the cardiac cycle, vibrations caused by the heart mechanical activity propagate through the chest, originating sounds

Please cite this article as: A. Dias Junior et al., Methods for reliable estimation of pulse transit time and blood pressure variations using smartphone sensors, Microprocessors and Microsystems (2016), http://dx.doi.org/10.1016/j.micpro.2016.06.001

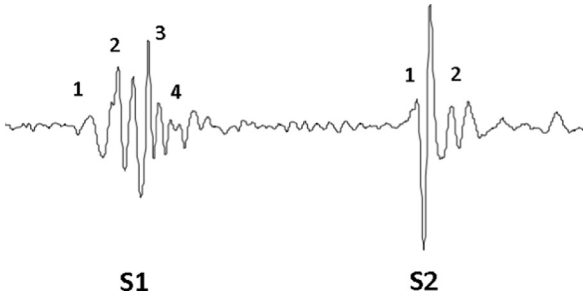

Fig. 1. Heart sounds S1 and S2. Adapted from [17].

that physicians have been using for centuries to assess the health of the heart. At least two heart sounds are very discernible on a healthy person. These sound events are usually referred as S1 and S2. S1 is believed to include four major components [17]: 1) The initial contraction of ventricles, which increases the ventricular pressure and accelerates the blood towards the atria; 2) The momentum of the moving blood as it forces the closure of the atrioventricular valves; 3) The oscillation of blood during the opening of aortic and pulmonary valves; and 4) The turbulence caused by the blood flowing through the Aorta. On the other hand, S2 includes two components that signals the closing of aortic and pulmonary valves. Fig. 1 shows a representation of the heart sounds S1 and S2 and their major components.

We are particularly interested in detecting the moment the blood leaves the heart as this is the genesis of the pulse pressure wave. This instant is marked by the third and fourth components of S1 and, by correctly delineating S1, it is possible to precisely compute PAT_0. We use the smartphone's internal microphone as a low cost phonocardiogram to perform this task, thus computing the PAT at the proximal point.

The PAT at the distal point is computed using the smartphone's camera as a photo-plethysmogram (PPG) sensor. PPG is a non-invasive method that uses optics to obtain information about the subcutaneous blood circulation [2]. PPG sensors gather the light transmitted through the living tissue and use the acquired signal to estimate arterial pulsatility and blood content. Our method uses the smartphone's flash light and camera to mimic a skin reflectance-based [18] PPG sensor. During the measurement, the subject holds his/her index fingertip over both the camera and the flash light. The light emitted by the LED is scattered by the living tissue, reflected by the digital phalange, and finally captured by the camera. The subtle changes in brightness due to the blood flow are used to reconstruct the blood pulse-wave signal. All signal acquisition, processing and delineation of the waveforms are performed in real-time to provide the user with visual and audio feedback. During the experiments we noticed that this feedback is essential to help the user to position the sensors, specially the microphone, at the right place. Moreover, audio-visual feedback enriches user experience, making the application more interactive and appealing.

This real-time feedback, nevertheless, puts an extra burden on the signal processing algorithms. To provide for a smooth execution during the real-time processing without negatively affecting the system robustness, we have splitted the signal processing step in two phases. Phase I performs a simple conventional filtering of the signals and a coarse delineation of the waveforms. This phase has two objectives: 1) extracting a clean signal with enough quality to be presented to the user; and 2) checking if the recorded signals have enough quality to be delineated in the second phase. During Phase I we just perform a preliminary analysis of the signals, not ensuring a perfect synchronization between the waveforms neither a precise delineation of their fiducial points.

The filtered samples are accumulated in a circular buffer during Phase I to be processed in the second phase. Once the required signal quality is met, the algorithms in Phase II further filter the signals, analyzing the entire buffer using advanced signal processing techniques. These algorithms rely on the fact that PPG and PCG are time-locked, as they are triggered by the same bio-event: the pumping of the heart. This multi-modal approach grants a robust and reliable delineation of the waveforms even using the inexpensive sensors present in stock smartphones. In Phase II, the precise fiducial points of the waveforms are detected and used to calculate PTT.

After computing the PTT, its value is fed to the blood pressure estimation model. Before starting using the application, the user must calibrate the model using a standard BP device, like the oscillometric-based devices largely available for ambulatory use. The calibration procedure requires the user to perform a PTT measurement using the smartphone. After the recording is done, the application asks the user to input a reference BP value collected with a standard BP device. The BP reference value is used to calibrate the PTTxBP model.

We experimented with PTTxBP models described in other works, like [3,5,11,19,20], some models cited in [21] and also with some generic regression models (linear, polynomial, etc.). Given the limited space and the fact that the blood pressure estimation model is not a new contribution of this specific work, but based on previous works, we ask the interesting reader to refer to those works for further information.

Fig. 2 shows a block diagram of the proposed two step real-time method for blood pressure estimation. The following section details each one of the blocks of the proposed solution.

3. Smartphone based signal acquisition and processing

Enabling cost-effective healthcare-based services on the mobile phones is the next step on telehealth systems. People are used to take their mobile phones everywhere, keeping them all day long in reach of their hands. This ubiquity makes mobile phones perfect to follow up patients at risk and to monitor sporadic vital signs deviations from the baseline. The biggest challenge, however, is how to deliver an effective healthcare solution using mobile phones without impacting neither the battery life nor the user experience due to the limited processing capabilities.

In this section we detail the acquisition and processing of PPG and PCG using the smartphones' baseline sensors. We focus on the Android operating system as it detained 82% of the market share in 2014 [22]. Most of the techniques presented here, nevertheless, are generic enough to be applied to other operating systems with little to no modification.

3.1. Photo-plethysmography acquisition

The proposed system uses the smartphone's camera as a PPG sensor to monitor the pulse waveform. Other mobile applications use the same principle to measure the subject's heart rate (HR), like the Azumio's Instant Heart Rate app [23]. Usually, the PPG signal is reconstructed from the individual frames of the camera and fed to a Fast Fourier Transform (FFT) algorithm that extracts the HR value. Frequency domain analysis, like FFT, may be robust enough to extract HR, but it is not sufficient for PTT calculation. In order to estimate blood pressure, we need to detect the exact moment the pressure pulse reaches the distal point (i.e. the fingertip), which requires the PPG signal to be precisely reconstructed and delineated in the time domain.

A major problem for PPG reconstruction arises when standard smartphones are used to capture the signal, specially Android-based ones. There is little hardware standardization among

Please cite this article as: A. Dias Junior et al., Methods for reliable estimation of pulse transit time and blood pressure variations using smartphone sensors, Microprocessors and Microsystems (2016), http://dx.doi.org/10.1016/j.micpro.2016.06.001

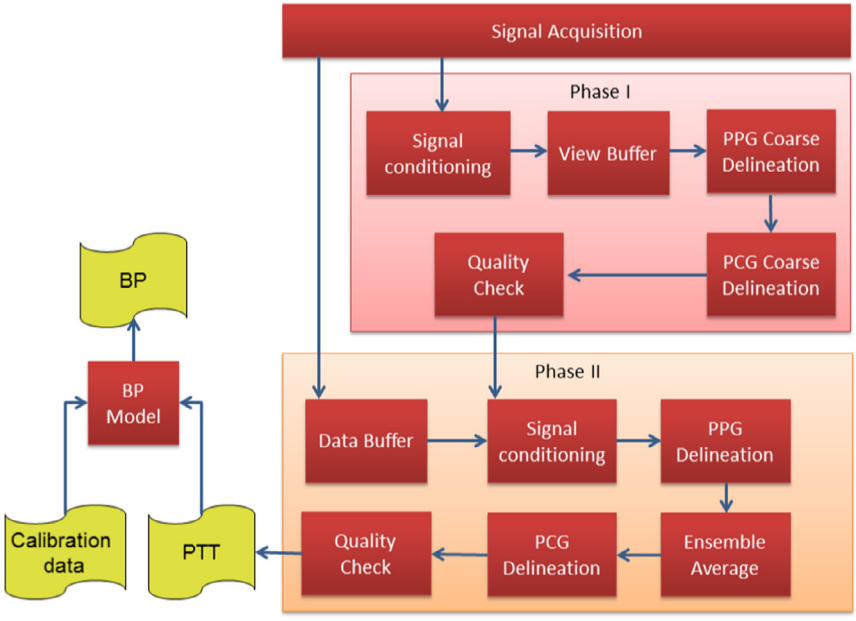

Fig. 2. Block diagram of the proposed two step real-time method.

Android devices and the operating system lacks support for frame temporization. Constant frame rates are not supported by the vast majority of devices and, as a consequence, the PPG reconstruction and delineation algorithm must take into account variable frame rates, specially those due to automatic exposure adjustment, and to restricted processing capabilities.

Automatic exposure (AE) allows the smartphone's camera to automatically determine the correct exposure time for compensating for poor lighting during recordings. Despite desirable in normal use, this feature is the main source of frame rates fluctuations and may distort the PPG signal when the pulse waveform is being acquired. Dynamic adjustment of exposure has two effects on the recorded PPG signal: 1) it changes the frame rate during the acquisition, distorting the signal time reference; and 2) it constantly changes the image brightness, distorting the amplitude of the signal. Hence, to get a non-distorted PPG signal, which is essential to correctly determining the fiducial points, the exposure time must be locked during the recordings.

We adopted a solution to prevent the AE feature to affect the measurements. After the user covers the lens to start the measure, we allow the AE feature to adjust the exposure for a few seconds (5 s, determined experimentally) and, then, lock the exposure to get a clean signal thereafter. With the AE feature locked, the average framerate observed for the smartphone model used during the experiments was 29.97 fps and the standard deviation for the worst experiment was 1.60 frames. It is worth noting that most of the PPG power is concentrated in low frequency components, in a very narrow band (from 5 to 11 Hz [2]), thus this sampling rate is sufficient to extract all the necessary information from the signal, as it is above the Nyquist rate, which is 22 samples/s.

With respect to the restricted processing capabilities, we used a frame buffer to guarantee that no frames are dropped by the operating systems during the demanding tasks and adopted a thread-based solution to take advantage of the multicore architectures while also preventing the user interface from hanging during the computations. The PPG value is therefore computed frame by frame by a handler thread, using the mean brightness in the red channel of the image. This value is then passed to the phase I algorithms for filtering and coarse delineation.

3.2. Phonocardiogram acquisition

Differently from the camera, Android audio recordings have a constant sample rate, which is selected from a set of valid frequencies before starting the acquisition. We use a sample rate of 44100 Hz as, according to the *Android 4.4 Compatibility Definition* [24], this is currently the only sample rate guaranteed to work on all devices. To reduce the required amount of computation we downsample the recording to 900 Hz before processing. This sample rate was selected for being higher than the Nyquist rate as the heart sound frequency spectrum is mainly located in the range from 10 Hz to 400 Hz [2]. Additionally, to guarantee we receive the raw samples from the microphone, we disabled the device's automatic gain control and noise reduction features.

PCG acquisition in Android systems, nevertheless, is not at all issue-free. First, all read operations involving the audio device are blocking and, hence, a working thread must be set up to prevent the system from hanging during recordings. Last, but not least, the Android's compatibility document only suggests that the hardware manufacturers reduce the audio latency, but does not require them to do it. Again, according to the *Android 4.4 Compatibility Definition* [24], the latency to get the first audio sample *should* be lower than 100 ms while in the rest of the recording, latency *should* be lower than 45 ms. These latency figures are just recommendations, not mandatory.

To circumvent the latency problem (and also to control the number of samples in the circular buffer during the first phase of the signal processing) we mark each sample with a timestamp that is relative to the moment the sampling started. Then we measure the latency using a simple procedure (described in Subsection 5.1) and add this value to the timestamp of the PPG samples. The premise of this solution is that the sample rate of the audio channel is stable, which we have confirmed during the experiments.

3.3. Phase I

As previously stated, the first objective of Phase I is to extract a clean signal, with enough quality to be presented to the user. Thus, during this first phase, the PPG and PCG input samples are filtered before storing them in a circular buffer. Filtering the acquired signals is fundamental for correctly extracting their fiducial

Please cite this article as: A. Dias Junior et al., Methods for reliable estimation of pulse transit time and blood pressure variations using smartphone sensors, Microprocessors and Microsystems (2016), http://dx.doi.org/10.1016/j.micpro.2016.06.001

Table 1
Filters specifications.

Name	Type	Order	Sample frequency (Hz)	Cut low (Hz)	Cut high (Hz)
PPG signal	High-pass IIR	6	30	0.5	•
PCG downsampling	Low-pass FIR	559	44100	•	450
PCG signal	Band-pass IIR	2	900	20	250
PCG envelope	Low-pass IIR	2	900	•	20

points. However, filtering usually incurs in a phase difference between the input and output signals. Sometimes, the filter phase response is non-linear (the phase shift is not directly proportional to the frequency) which may result in distortions that have an impact on the accuracy of the fiducial points detection. Here, we use two types of digital filters: Finite Impulse Response (FIR) and Infinite Impulse Response (IIR) [25]. In the case of linear phase FIR filters, the phase difference from the input signal can be easily compensated by subtracting a constant value from the sample timestamp. IIR filters, on the other hand, usually have non-linear phase response, which causes distortions in the signal. However, IIR filters are computationally more efficient then FIR filters which is a significant advantage when processing capability is restricted.

We opted to use IIR filters whenever possible to reduce the processing requirements of the system. The distortions caused by the phase non-linearity do not have significant impact on the user feedback and, hence no effort was made to eliminate them during Phase I. In Phase II, nevertheless, the distortions may affect the PTT calculation and then we use techniques that sacrifice the real-time processing for linearity, as it will be presented in the next subsection. Table 1 shows the design parameters for the filters used in phase I and phase II.

Two circular buffers were defined for storing the values of each bio-signal (two for PPG and two for PCG). The first buffer (*view buffer*) holds the data that will be presented to the user in real-time during Phase I. The second buffer (*data buffer*) contains the data used to calculate PTT in phase II. This separation between *view* and *data* buffers improves the real-time data processing, since the data presented to the user does not require to be precise, but just representative enough to give the user a quality feedback. The real-time processing over the *view buffer* is efficient especially because of two factors:

1. The *view buffer* is smaller than the *data buffer*, since just a few heart cycles are sufficient to provide the user with audio-visual feedback;
2. All filtering, except for the *PCG Downsampling*, is performed by causal IIR filters, since light distortions in the user feedback do not interfere with usability.

Every time a new PPG sample is calculated from the camera frames, a pair $< value, timestamp >$ is inserted into the PPG *data* and *view* buffers. The value added to the *data buffer* is inserted without any filtering or processing, while the value inserted into the *view buffer* is filtered using the *PPG Signal* filter presented in Table 1. Since it is an IIR filter, the data will be lightly distorted, but without impacting the PTT calculation, which uses the *data buffer* in Phase II.

The samples from the audio device, on the other hand, are downsampled in real time using the *PCG Downsampling* filter before being inserted into the buffers. The *PCG Downsampling* filter has a linear phase and downsamples the audio signal from 44100 Hz to 900 Hz, while also works as a low-pass filter, attenuating components above the Nyquist Frequency at the same time. Before being inserted into the *view buffer*, the PCG samples are further processed to create an envelope that allows the user to identify the heart sounds S1 and S2. First, the *view* samples are filtered by the *PCG Signal* filter. Then, the samples are normalized to the interval [0.00, 1.00] and used to calculate the energy, using the formula presented in Eq. (2). Finally, the samples are filtered using the *PCG Envelope* filter, which creates an envelope of the signal.

$$E(t) = -x(t)^2 . \log(x(t)^2) \tag{2}$$

where $E(t)$ is the energy at time t and $x(t)$ is the filtered sample value at time t.

Besides filtering and inserting data into the buffers, Phase I also coarsely delineates and analyzes the signals to trigger the execution of Phase II algorithms. Listing 1 presents a high level algorithm for this task.

PCG data acquisition is performed precisely at 44100 Hz and the signal is downsampled to 900 Hz before inserting into the circular *data* and *view* buffers. The PCG *data buffer* was designed to hold 14 s of samples while the *view buffer* is capable of storing 4 s. Once filled, the buffers start discarding the oldest samples every time a new sample is inserted. PPG, on the other hand, has a variable frame rate and automatic sample discarding based on the number of samples is not possible. Hence, before analyzing the signals, PPG and PCG buffers must be synchronized. This task is performed by the alignment procedure, executed at line 6 of Listing 1. Since the sample rate of PCG is much higher than that of PPG, the synchronization is performed by getting the first timestamp from the beginning of the PPG buffer and discarding all data that precedes it in the PCG buffer.

After aligning the PPG and PCG buffers, the PPG signal stored in the *view buffer* is delineated (line 7 of Listing 1). The objective of the delineation phase is to detect the moment the pulse wave reaches the finger. This moment is marked by the onset of the PPG pulse waveform and is determined using the following steps:

1. The minima of the waveform are detected using the derivative of the signal;
2. The detected minima, so-called feet, are analyzed according to their amplitudes. All points that do not fall into the valid range (that are determined experimentally) are discarded;
3. The time difference between two given feet is checked for significant deviations from the mean. If two feet are too close to each other, their neighbors are checked, trying to solve these discrepancies. If removing one of them solves the deviation, that foot is discarded;
4. The remaining points are checked for zero-crossing points between them. All PPG wave feet must be separated by two zero-crossing points. If this condition is not met for any given two feet, the one with lower amplitude is kept and the other one is discarded.

Once the feet of the pulse waves are detected, they are checked for stability (line 8 of Listing 1). If the longest beat is greater than 1.5 times the shortest beat, probably the delineation algorithm missed one beat or wrongly detected a pulse wave onset. Otherwise, the detected points time difference is stable and the PPG delineation is considered good enough.

The next step is to delineate the PCG signal (line 9 of Listing 1). PCG signal is significantly more difficult to be delineated than the PPG because of the noise captured by the smartphone's microphone. However, the complexity of this task is attenuated as we

Please cite this article as: A. Dias Junior et al., Methods for reliable estimation of pulse transit time and blood pressure variations using smartphone sensors, Microprocessors and Microsystems (2016), http://dx.doi.org/10.1016/j.micpro.2016.06.001

```
FUNCTION Phase_I
  TRIGGER: A new sample is inserted into
           the PPG buffer
BEGIN
  if (PPG dataBuffer is full) then
    align PPG and PCG data buffers
    delineate PPG view buffer
    if (PPG delineation is good enough) then
      delineate PCG view buffer guided by PPG
      if (PCG delineation is good enough) then
        call Phase_II
      endif
    endif
  endif
END
```

Listing 1. Phase I algorithm.

already have information regarding the individual heart beats, extracted during the PPG delineation. In a normal condition, an onset in the PPG signal must follow every S1 sound event in the PCG signal. For the coarse delineation executed in Phase I, we check for pairs of peaks in the PCG envelope (S1 and S2) that are way above the average signal value. If a pair of peaks within a valid time difference precedes each one of the PPG onsets, the PCG signal has enough quality to be processed and the second phase of the analysis is triggered.

3.4. Phase II

The algorithms in Phase II are very similar to the ones in Phase I except for the fact that they use the bigger *data buffers* instead of the *view buffers*. There are some important differences, nevertheless, that significantly improve the quality of delineation in the second phase.

First, the IIR filters are applied over the *data buffers* in both directions during Phase II, using a forward-backward scheme. This results in a non-causal filter that is realizable just because all samples have already been acquired and are stored in the buffers, ready to be processed. Using this technique, the result is a signal without the phase distortions that would impact on the fiducial points determination.

Second, we use a more robust technique to delineate the PPG and PCG signals. The technique is based on ensemble averaging the signals to remove noise that is unrelated to the heart beat. This technique relies on the fact that over short time windows, the PCG and PPG fiducial points may be considered time-locked. Solá [2] used ensemble average (EA) to filter the ICG signal using ECG R-wave peaks as triggers. The author demonstrated that using EA corresponds to applying a very narrow band-pass filter with central frequencies defined by the heart rate frequency and its harmonics. Here we calculate the EA using the onsets of the PPG signal as trigger points, since this signal is, in general, less noisy than the PCG.

Let τ_i be the timestamp of the ith onset of the PPG wave and N be the number of detected onsets during the PPG delineation of the *data buffer* in Phase II. The ensemble average of the signal, $\hat{s}$, is computed over the original signal, s, using the formula presented in Eq. (3).

$$\hat{s}(t) = \frac{1}{N}\sum_{i=1}^{N} s(t+\tau_i) \tag{3}$$

where $t \in [0, T)$ and T is the heart beat period. Fig. 3 illustrates the computation of the ensemble average.

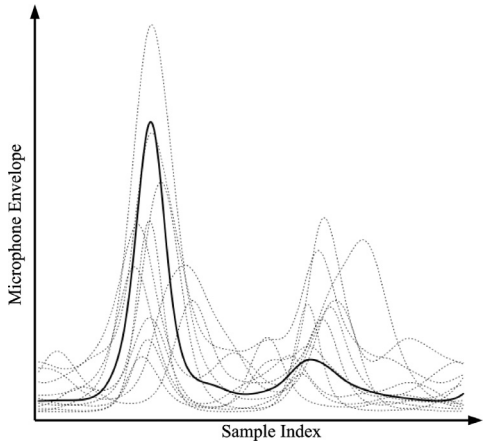

Fig. 3. PCG filtering using the ensemble average technique

By computing $\hat{s}$ using Eq. (3), we obtain a denoised version of a single heart beat of s, averaged over N heart beats of that signal. After applying this technique over both the PPG and PCG, we have two options for calculating PTT:

1. delineate both $\hat{s}_{PPG}$ and $\hat{s}_{PCG}$ and calculate the PTT using the detected fiducial points;
2. use $\hat{s}_{PPG}$ and $\hat{s}_{PCG}$ as template waveforms to delineate the original signals, s_{PPG} and s_{PPG}, and calculate N PTTs for the N heart beats.

We opted to use the second option as it allows tracking beat-to-beat variations of PTT caused by special situations like standing up, or performing the Valsalva-Weber maneuver [26]. Besides, by averaging the PTT values over several beats we increase the time resolution of the measurements, compensating for the sampling rate of the camera.

4. Further improvements on the method

The proposed method, as presented in the previous sections, is capable of measuring the PTT in a reliable and robust way. However, the process of correctly positioning the smartphone's sensors, especially the microphone, may be tedious and frustrating if no proper feedback is provided to the user. The strategies described in this section offer further improvements on the user experience in addition to the visual information provided by the real-time chart described in Section 2. Moreover, the additional steps described here also have a positive impact on the method robustness, es-

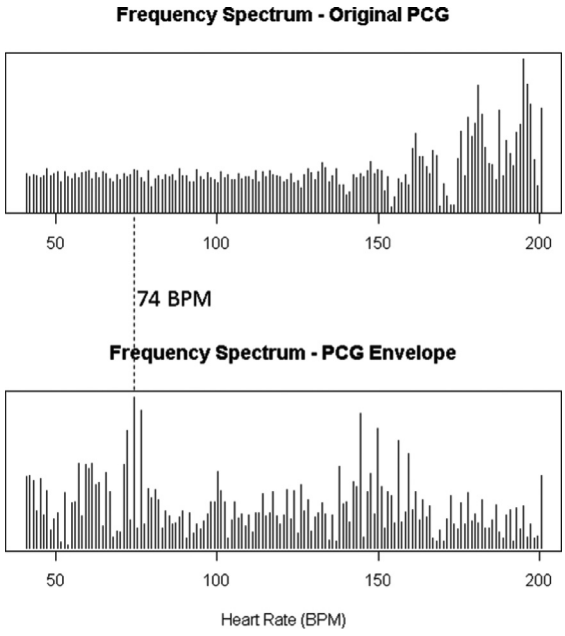

Fig. 4. Comparison between the frequency spectrum calculated from original PCG and from the PCG envelope.

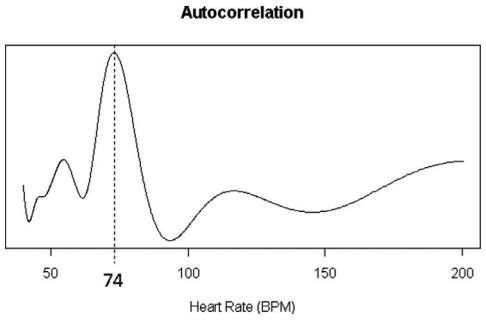

Fig. 5. Using the auto-correlation value to compute HR

pecially with respect to the frame rate fluctuations of the camera recordings.

This section is divided into three subsections. First, we present a simple way of improving the user experience by measuring and presenting the heart rate (HR) extracted from the sound captured using the microphone. This feature is useful to help the user to find the proper place to position the microphone on the chest. We also compare frequency domain analysis (Fast Fourier Transform - FFT) with time domain analysis (a naive yet effective time-based auto-correlation algorithm) with respect to robustness, computation time performance and memory usage. Second, we propose a way of using the computed HR to compensate for the camera frame rate variations. Since the camera is the weakest link in the sensor chain, improving its reliability is important to increase the exactness of the method. Finally, we show how to use the obtained HR to assess and improve the quality of the delineation of both the PPG and PCG signals.

4.1. Capturing the HR from the PCG

Extracting the HR from the PPG, even when acquired using a standard smartphone camera, is a straightforward process and several commercial applications are available to perform this task. The PPG signal obtained from the camera usually presents low noise and, therefore, the most prominent frequency component computed by the FFT corresponds to the HR value. To measure the HR using this setup is as simple as applying the FFT on the signal window and determining the frequency component with the maximum magnitude.

The same task when performed over the PCG, nevertheless, may present some difficulties. First, the raw PCG is usually subject to a variety of noises that might influence the FFT results. Moreover, the energy of the raw PCG signal is dispersed throughout the spectrum due to the diversity of frequency components of the heart sounds, making it more difficult to define the correct HR. One way to circumvent this problem is to apply the FFT over the PCG envelope calculated using Eq. (2) instead of using the original PCG signal. Fig. 4 shows a comparison between the frequency spectrum calculated from the original (filtered) PCG and the PCG envelope over the same recording of 50 seconds of heart sounds. As can be seen in that figure, the HR frequency is easier to be extracted from the spectrum calculated using the PCG envelope than from the original PCG frequency spectrum.

Alternatively, the HR can be computed using a value that is proportional to the auto-correlation of the signal, using the simple (and naive) time domain approach described by Eq. (4).

$$A(l) = \sum_{t=0}^{W-l} x(t) \times x(t+l) \tag{4}$$

where $A(l)$ is a value that is proportional to the auto-correlation of the signal x at lag l; W is the size of the window where the auto-correlation is being computed; and $x(t)$ is the PCG envelope value at time t.

The lag value with the maximum correlation can be finally computed using the expression presented in Eq. (5).

$$Lag_{max} = \arg\max_{l \in [L_1, L2]} A(l) \tag{5}$$

where L_1 and L_2 are respectively the minimum and maximum lags for a valid HR value. Fig. 5 shows the curve computed using Eq. (4) for the same PCG envelope used to build the spectrograms of Fig. 4.

When compared to the FFT approach, the main advantage of computing the HR value using the time domain analysis described by Eq. (4) is that it requires less memory than FFT algorithms. FFT algorithms compute the frequency components using complex numbers and, therefore, they require three memory vectors with capacity proportional to the number of samples of the signal (one for the original signal, which in this application cannot be overwritten, the other two to store the real and imaginary parts of the result). The time domain approach does not need any other vector apart from the original signal being, therefore, more memory efficient.

On the other hand, computing the FFT for a given vector is usually less computationally demanding than computing the auto-correlation for the same vector using the method described in Eq. (4). While the FFT has a time complexity of $O(n \log n)$ for n samples, the auto-correlation would be computed in $O(n \times l)$ using that method, where L is the size of the lag window. To compute the auto-correlation for the entire vector, therefore, the time complexity will be $O(n^2)$, as $l \approx n$.

This time complexity can be drastically reduced, nevertheless, if the size of the lag window is constant. Moreover, the smaller the window, the better the auto-correlation-based algorithm performs in comparison to the FFT, as it can be seen in Fig. 6. When the size of the lag window is sufficiently small, the naive auto-correlation algorithm described by Eq. (4) requires as much time as the FFT algorithm to compute the HR, but using less memory.

The behavior presented in Fig. 6 is used to improve the performance of the proposed method. We decided to use the FFT approach during Phase I, as at that phase the buffer is smaller than

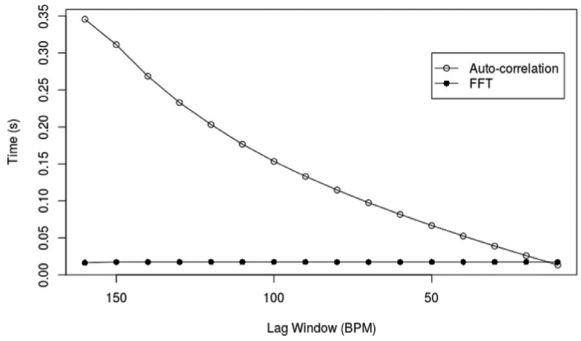

Fig. 6. Time to compute the HR versus the size of the window.

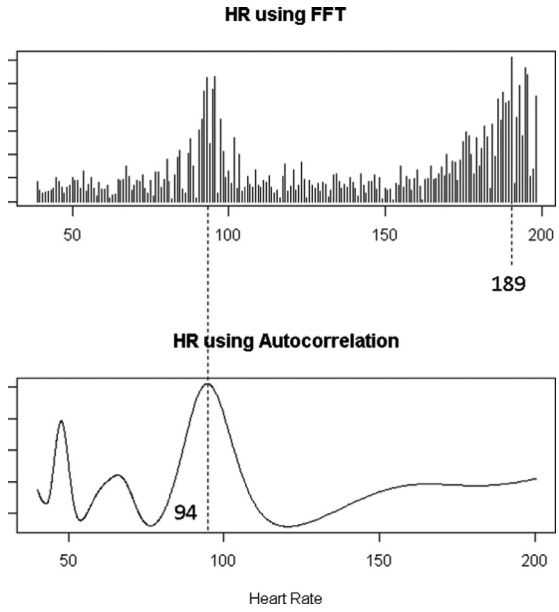

Fig. 7. Wrong computation of HR by the FFT.

in Phase II (4s of samples against 14 s) and, hence, the impact of duplicating the buffer would not be significant. More importantly, during Phase I we do not have any information on what is the user current heart rate and, therefore, the HR detection algorithm should search for the HR component through the entire valid range, which is fixed between 40 and 200 beats per minute. The auto-correlation algorithm performs poorly on such a wide window.

During Phase II, nevertheless, we opted to use the simple auto-correlation approach for two reasons. First, the auto-correlation requires less memory to compute the HR than FFT-based algorithms. Second, the lag window to be considered is significantly narrower during Phase II than during the first phase. The reason is that the HR computed in Phase II should be similar to the one computed during Phase I. We considered a window of 10 beats per minute during Phase II centered on the HR computed during Phase I ($HR_I \pm 5$ b.p.m).

Finally, It is worth noting that the auto-correlation algorithm has been proven to be more robust than the FFT during the experiments. We have noticed that, when the time between S1 and S2 is around half the period of the entire beat, the FFT-based algorithm may yield an HR that is twice the actual rate. The auto-correlation, on the other hand, delivers proper results even in this case. This behavior is depicted in Fig. 7, where the FFT maximum magnitude component is twice the actual Heart Rate, which was computed correctly by the auto-correlation algorithm.

4.2. Compensating for frame rate fluctuations

Besides improving user experience, the HR can also be used to compensate for frame rate fluctuations during the camera acquisition. In the following analysis, we use the general formula to calculate HR, in beats per minute (bpm), expressed in Eq. (6).

$$HR = 60 \times SR \times factor \tag{6}$$

where SR is the signal sample rate and $factor$ is defined by the method used to extract the HR, as defined by Eqs. (7) and (8).

$$factor_{fft} = \frac{K_{max}}{N} \tag{7}$$

$$factor_{ac} = \frac{1}{Lag_{max}} \tag{8}$$

where K_{max} is the index of the maximum magnitude frequency component as calculated by the FFT over a vector of length N, and Lag_{max} corresponds to the lag value of maximum positive correlation, calculated using Eq. (4).

Since both PPG and PCG signals are generated by the same cardiac event, they are synchronized and, therefore:

$$HR_{PPG} = HR_{PCG} \tag{9}$$

Substituting Eq. (6) in (9), we obtain:

$$60 \times SR_{PPG} \times factor_{PPG} = 60 \times SR_{PCG} \times factorPCG \tag{10}$$

However, as stated in Section 3.2, the PCG sample rate (SR_{PCG}) is well known and does not vary during the acquisition. Therefore, by simple manipulation of Eq. (10), we obtain the formula to calculate the actual sample rate of the camera, based on the PCG sample rate, which is presented in Eq. (11).

$$SR_{PPG} = \frac{SR_{PCG} \times factor_{PCG}}{factor_{PPG}} \tag{11}$$

The actual SR_{PPG}, calculated using Eq. (11), provides a more solid basis to determine the time of occurrence of the PPG signal events. Moreover, the main benefit of calculating this value is it can also be used to check the quality of the PPG acquisition: since the timestamps are not provided by the operating system, if the actual SR_{PPG} is significantly different from the SR calculated during the acquisition, the PPG wave is probably too distorted to be used for PTT computation and the entire signal window should be discarded.

4.3. Using HR to support the delineation

Additionally, the HR (calculated using the FFT in Phase I or using the auto-correlation in Phase II) can also be used to support the delineation algorithm in both phases. Instead of calculating the mean difference between the onsets of the PPG to validate the position of the wave feet, as it was described in Subsection 3.3, the HR can be used as a reference. If two feet are too close to each other when compared to $\frac{1}{HR}$, their neighbors are checked, trying to solve these discrepancies. If removing one of them solves the deviation, that foot may be safely discarded.

After the delineation, the HR also provides a way to assess the quality of the delineation. If the longest delineated beat is more than 1.5 times $\frac{1}{HR}$, the delineation is probably wrong and should not considered to be good enough to calculate the PTT.

5. Experiments

We performed a series of experiments to evaluate the proposed filtering and delineation algorithms. It is worth noting that the experiments are not intended to validate the use of PTT as a surrogate marker for blood pressure as this issue has been addressed

Please cite this article as: A. Dias Junior et al., Methods for reliable estimation of pulse transit time and blood pressure variations using smartphone sensors, Microprocessors and Microsystems (2016), http://dx.doi.org/10.1016/j.micpro.2016.06.001

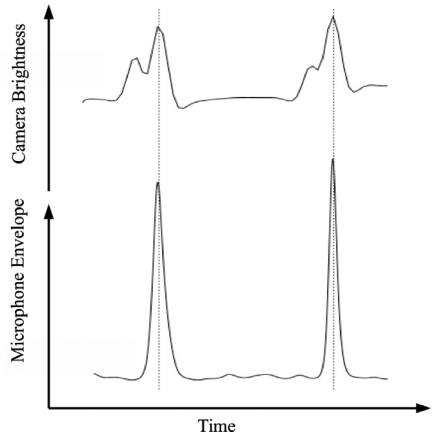

Fig. 8. Synchronization experiment results.

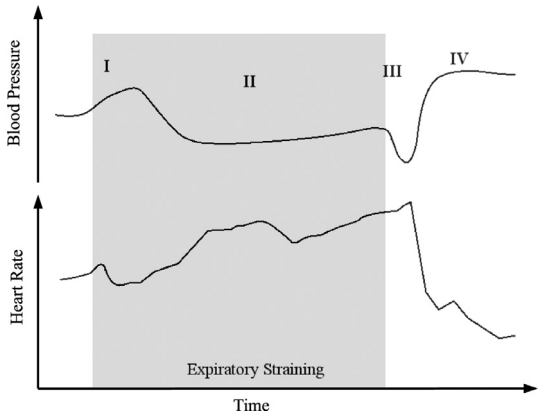

Fig. 9. Normal behavior during the Valsalva-Weber Maneuver. Adapted from [26].

by several previous works. We aim at validating our solution with respect to three major aspects: 1) the synchronization between PPG and PCG signals; 2) its capability of tracking beat-to-beat PTT changes; and 3) the accuracy in determining the waveforms fiducial points.

Experiments were performed using a Samsung S4 smartphone running Android 4.4 operating system. Data was collected and processed using a hybrid application developed in Java and C. We opted to use C in the signal processing algorithms because native code presents better time performance than pure Java applications. Despite all results presented in this section were obtained using solely the mobile application, for convenience we used the software Matlab [27] to create the plots.

5.1. Synchronization between PCG and PPG

As the PCG and PPG signals are acquired by different subsystems of the smartphone, it is necessary to check whether they are being generated in perfect synchronization. If the signals are not correctly aligned in time, the accuracy of the obtained PTT value would be compromised. A simple procedure was adopted to evaluate the synchronization between PCG and PPG: we applied a sequence of tappings on the smartphone, each tap completely covering the camera lenses and generating a sound at the same time. If data acquisition and synchronization are correctly performed by the application, the generated PPG and PCG waveforms should present a perturbation around the same time instant.

This experiment was performed several times to make sure fluctuations on the frame rate and other transitory conditions do not affect the synchronization between the signals. During its execution, we have noticed that the camera waveform peak always happened two frames before the microphone peak. In order to synchronize both signals, we added a constant delay to the timestamp of each camera sample. The result of the experiments, after this latency problem correction is presented in Fig. 8. With this correction, the waveforms present perfect synchronization, therefore showing that the adopted synchronization scheme is suitable to reliably calculate PTT.

5.2. Tracking of beat-to-beat PTT changes

In order to evaluate the capability of the developed solution to track beat-to-beat variations of BP and HR, it is required that a disturb is induced on the user's cardiovascular system, thus generating observable changes on the monitored signals during the PCG and PPG acquisition. Usually, these changes in BP and HR are created by submitting the user to a series of physical exercises. However, the solution we propose in the present work is not suitable for use during physical activities as it requires the user to stand still or seat in a specific position, preferably on a quiet environment. The movement of the body, during the exercises would add too much noise on the PCG acquisition, specially due to the microphone-skin friction. Hence, we opted to employ the Valsalva-Weber maneuver to produce the changes on the monitored signals.

The Valsalva-Weber maneuver consists in asking the patient to perform a full inspiration followed by a sustained forced expiration against the closed glottis, nose, and mouth. After a few seconds, the expiration restraint is loosened and the patient should try to breath as normally as possible.

During the execution of Valsalva-Weber maneuver, it is possible to observe four phases in which acute changes in HR and BP occur [26], as depicted in Fig. 9. During the initial inspiration (phase I), the HR shortly reduces and a sudden increase in systolic BP is perceived; as the subject maintains the expiratory strain (phase II), HR progressively increases, while Systolic BP decreases in a similar fashion; when breath is finally released (phase III), HR reaches its peak and BP fall shortly to its minimum level; the recovering phase (phase IV) is marked by a progressive reduction of HR, which reaches its minimum value before returning to the basal state. BP value also presents a progressive increase, with an overshoot before returning to pre-maneuver levels.

Three subjects were submitted to the Valsalva-Weber maneuver during the experiments: one female (subject 1) and two male (subjects 2 and 3). Subject 1 does not perform any regular physical activity, presenting a high basal HR of around 100 bpm. Subject 2 undergoes moderate physical activity twice a week, and Subject 3 is an active sportsman who performs intense training regularly. Fig. 10 presents the waveforms for HR and relative (uncalibrated) BP for these subjects. Upon inspection of that figure, the four expected phases for both HR and BP curves are identified. The curves for the three subjects match the template of Fig. 9.

5.3. Fiducial points classification accuracy

We have also checked the delineation accuracy of the proposed methods. For the same three subjects for which the results were presented in Section 5.2, PPG and PCG waveforms were delineated both automatically using the proposed algorithms, and manually by inspecting the raw waveforms before any processing. Manual PCG delineation was performed using the template waveform of Fig. 1 and, as previously stated, we used the third component of S1 as the proximal point. PPG manual delineation was performed using the intersecting tangent method [28] which defines the onset of the pulse wave as the intersection point between a tangent line through the initial systolic upstroke of the PPG waveform and

Please cite this article as: A. Dias Junior et al., Methods for reliable estimation of pulse transit time and blood pressure variations using smartphone sensors, Microprocessors and Microsystems (2016), http://dx.doi.org/10.1016/j.micpro.2016.06.001

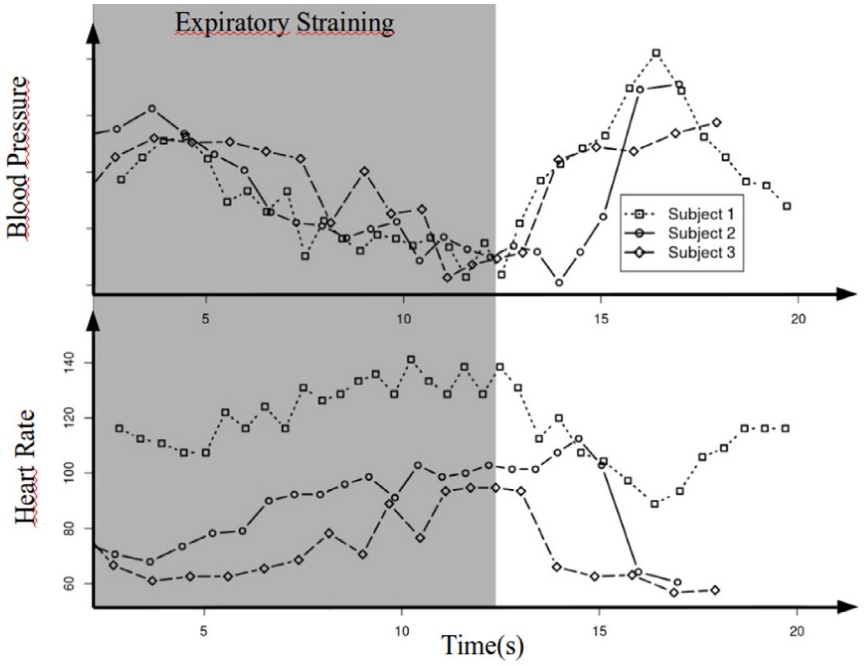

Fig. 10. HR and BP curves obtained during the experiments.

Table 2
Difference between automatic and manual delineation.

	PCG S1 (ms)		PPG onset (ms)		PTT (ms)		
	Max	Mean	Max	Mean	Max	Mean	Mean Perc.
Subject 1	2.72	1.40	6.67	5.00	8.60	5.61	2.55%
Subject 2	5.49	2.27	13.30	5.14	11.76	5.19	2.04%
Subject 3	13.38	4.04	13.33	4.92	21.61	6.98	3.00%
Average	7.20	2.57	11.10	5.02	13.99	5.93	2.53%

a horizontal tangent line passing over the minimum point of the same wave. The maximum and mean difference between the manual and automatic determination of the points were recorded and the results are presented in Table 2.

During the compilation of Table 2 data, we have noticed that Subject 2 was presenting a high maximum error for both PCG and PTT values. Upon careful inspection of the waveforms, we have found out that this high error figure was due to a misclassification during the manual analysis of the data. A spurious sound was captured by the microphone, most probably due to an involuntary movement during the acquisition. This sound was mistaken during the manual PCG delineation by an S1 event and the subsequent peak, which was the real S1 peak, was assumed to be an S2 event. The automatic delineation algorithm, nevertheless, was able to correctly identify the actual S1 peak as it uses the PPG waveform and the time intervals to support the delineation. Fig. 11 shows the misclassification and also the correct analysis of the waveform. After correcting this inspection, the manual delineation was corrected and the errors were recalculated.

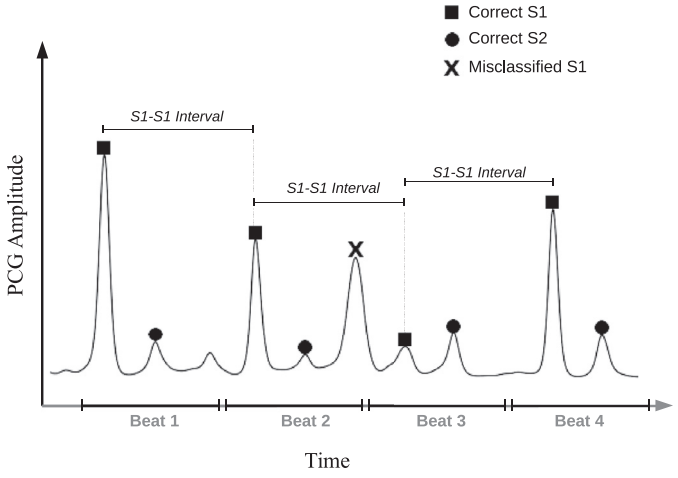

Fig. 11. Misclassification of manual delineation.

6. Discussion

The experiments presented in Section 5 aimed at validating the solution with respect to three major aspects: 1) the synchronization between PPG and PCG signals; 2) its capability of tracking beat-to-beat PTT changes; and 3) the accuracy in determining the waveforms fiducial points.

A simple procedure was adopted to evaluate the first aspect (i.e. the synchronization between PCG and PPG): we applied a sequence of tappings on the smartphone, each tap completely covering the camera lenses and generating a sound at the same time. We expected the perturbations to be present around the same time instant for both PPG and PCG signals. A delay corresponding to two camera frames was found in the PCG when compared to the PPG signal, showing that the audio subsystem of the smartphone takes some time to start the acquisition of samples after the command has been issued. This delay was consistent across several experiments and was compensated by adding a constant value to the timestamp of each camera frame, therefore synchronizing the signals. The probable cause of this behavior is the lack of support for real-time audio by the Android operating system. However, we have analyzed features of devices designed by different brands (Apple, Samsung, Sony, Nokia, etc.) and with different Operating Systems (Android, Windows, iOS) and realized that the support for real-time audio and constant frame rates by the camera, if

not yet supported, are on the road-map for all devices and OSs. Multimedia applications are the main driver behind this advance, but e-health solutions would benefit from these features as well. If the obtained results were not so consistent as they were, we had the option of analyzing the JPEG stream provided by the video recording subsystem. Video recording is performed directly by the hardware of the device in most (if not all) smartphones and, thus, it is not subject to the delays introduced by the OS. We decided not to use the JPEG stream because it would sacrifice some real-time features of the application.

To assess the accuracy of the method and its capability of tracking instant variations of PTT, we submitted three subjects to the Valsalva-Weber maneuver, inducing acute changes in their BP and HR. We compared the obtained results with the expected templates and their behavior matched, as expected. This result indicates that the applications is capable of detecting beat-to-beat variations of PTT. We checked the accuracy of the delineation (and the accuracy of PTT computation) by comparing the entire record of PTTs for each subject, as calculated by the application, to the PTTs computed manually using standard delineation methods. The results were promising showing a mean deviation from the manual computation never higher than 3.00%. We noticed that the fiducial points determined automatically for a few beats in each record presented significant differences from the values obtained manually, but even with these discrepancies the mean error was low, showing that employing the average of N beats had, indeed, contributed to the accuracy. At this point, it is not clear if these discrepancies are due to the automatic delineation or the manual determination of the fiducial points. We intend to compare the results obtained by the application to other automatic instruments to further clarify these findings.

As a final remark, it was clear that the use of the PCG template created from the Ensemble Average to delineate the individual beats of the PCG is a powerful technique. Since the acoustic disturbances are usually uncorrelated to the signal being measured, the fluctuations caused by them are attenuated by the EA resulting in a more robust delineation algorithm. This behavior is depicted in Fig. 11, where it is shown how the proposed solution handles room noise gracefully.

7. Conclusion

In this paper, we have presented methods for reliable estimation of Pulse Transit Time, and hence Blood Pressure, using only mobile phones with stock configuration. The main contributions of the present research so far are: 1) a low profile two step processing method that supports real-time acquisition and processing of PCG and PPG waveforms, providing the user with audio-video feedback and enhancing his/her experience with the mobile application; and 2) a robust method for filtering PPG and PCG signals using the ensemble average technique to create a template waveform that is used to guide the delineation of the less-than-ideal signals acquired using inexpensive sensors. Besides these two main contributions, to the best of our knowledge, this is the first time short-term variations of BP are tracked beat-to-beat based solely on phonocardiogram and photoplethysmogram, both acquired using inexpensive sensing and analysis circuitry.

We have validated the solution across subjects using the Valsalva-Weber maneuver to induce acute beat-to-beat variations of BP and HR. The waveforms obtained during the experiments match the expected template for both signals. Thus, these results indicate that our proposed methods are promising and suitable, in principle, for ambulatory monitoring of short-term variations in blood pressure values using just smartphone devices. Future investigations will be conducted to compare the obtained results with standard PTT acquisition equipment during the execution of daily activities to characterize the accuracy of the approach.

Acknowledgment

This work has been partially supported by a CAPES Scholarship (grant no. 2171-13-9, the ObeSense (no. 20NA21 143081), and BodyPoweredSenSE (no.20NA21 143069) RTD projects, evaluated by the Swiss NSF and funded by Nano-Tera.ch with Swiss Confederation financing.

References

[1] World Health Organization, A Global Brief on Hypertension, Technical Report, World Health Organization, Geneva, Switzerland, 2013.
[2] J.M. Solà i Carós, Continuous non-invasive blood pressure estimation, ETH Zürich, 2011 Ph.D. thesis.
[3] M. Banet, M. Dhillon, D. McCombie, Body-worn system for measuring continuous non-invasive blood pressure (cnibp), 2010, US Patent App. 12/650,383.
[4] J. Sola, M. Proenca, D. Ferrario, J.-A. Porchet, A. Falhi, O. Grossenbacher, Y. Allemann, S. Rimoldi, C. Sartori, Noninvasive and nonocclusive blood pressure estimation via a chest sensor, Biomed. Eng. IEEE Trans. 60 (12) (2013) 3505–3513, doi:10.1109/TBME.2013.2272699.
[5] V. Chandrasekaran, R. Dantu, S. Jonnada, S. Thiyagaraja, K. Subbu, Cuffless differential blood pressure estimation using smart phones, Biomed. Eng. IEEE Trans. 60 (4) (2013) 1080–1089, doi:10.1109/TBME.2012.2211078.
[6] R. Sethi, J. Watson, Systems and methods for non-invasive blood pressure monitoring, 2010, WO Patent App. PCT/IB2009/006,136.
[7] G. Kuchler, Noninvasive blood pressure determination method and apparatus, 2008, US Patent 7,374,542.
[8] D. McCombie, A. Reisner, H. Asada, Motion based adaptive calibration of pulse transit time measurements to arterial blood pressure for an autonomous, wearable blood pressure monitor, in: Engineering in Medicine and Biology Society, 2008. EMBS 2008. 30th Annual International Conference of the IEEE, 2008, pp. 989–992, doi:10.1109/IEMBS.2008.4649321.
[9] P. Shaltis, A. Reisner, H. Asada, Wearable, cuff-less ppg-based blood pressure monitor with novel height sensor, in: Engineering in Medicine and Biology Society, 2006. EMBS '06. 28th Annual International Conference of the IEEE, 2006, pp. 908–911, doi:10.1109/IEMBS.2006.260027.
[10] Casio Computer Co. Ltd., Module no. 2196, 1993,
[11] D. McCombie, M. Dhillon, M. Banet, System for calibrating a ptt-based blood pressure measurement using arm height, 2014, US Patent 8,672,854.
[12] A. Hennig, A. Patzak, Continuous blood pressure measurement using pulse transit time, Somnologie - Schlafforschung und Schlafmedizin 17 (2) (2013) 104–110, doi:10.1007/s11818-013-0617-x.
[13] L. Dennison, L. Morrison, G. Conway, L. Yardley, Opportunities and challenges for smartphone applications in supporting health behavior change: qualitative study, J. Med. Internet Res. 15 (4) (2013) e86.
[14] M. Kirwan, C. Vandelanotte, A. Fenning, M.J. Duncan, Diabetes self-management smartphone application for adults with type 1 diabetes: randomized controlled trial, J. Med. Internet Res. 15 (11) (2013) e235.
[15] G. Figueras, V. Parra, M. Huerta, A. Marzinotto, R. Clotet, R. González, A. Moreno, K. Pinto, D. Rivas, R. Alvizu, et al., Smartphone application for quantitative measurement of parkinson tremors, in: VI Latin American Congress on Biomedical Engineering CLAIB 2014, Paraná, Argentina 29, 30 & 31 October 2014, Springer, 2015, pp. 785–788.
[16] A. Dias Junior, S. Murali, F. Rincon, D. Atienza, Estimation of blood pressure and pulse transit time using your smartphone, in: Digital System Design (DSD), 2015 Euromicro Conference on, 2015, pp. 173–180, doi:10.1109/DSD.2015.90.
[17] C. Ahlström, Nonlinear Phonocardiographic Signal Processing [Elektronisk resurs], Institutionen för Medicinsk Teknik, 2008.
[18] Y. Mendelson, B. Ochs, Noninvasive pulse oximetry utilizing skin reflectance photoplethysmography, Biomed. Eng. IEEE Trans. 35 (10) (1988) 798–805, doi:10.1109/10.7286.
[19] H. Gesche, D. Grosskurth, G. Kchler, A. Patzak, Continuous blood pressure measurement by using the pulse transit time: comparison to a cuff-based method, Eur. J. Appl. Physiol. 112 (1) (2012) 309–315, doi:10.1007/s00421-011-1983-3.
[20] J.Y.A. Foo, C.S. Lim, P. Wang, Evaluation of blood pressure changes using vascular transit time, Physiol. Measur. 27 (8) (2006) 685.
[21] D. Buxi, J.-M. Redouté, M.R. Yuce, A survey on signals and systems in ambulatory blood pressure monitoring using pulse transit time, Physiol. Measur. 36 (3) (2015) R1.
[22] Gartner, Inc., Gartner says sales of smartphones grew 20 percent in third quarter of 2014, 2014.
[23] Azumio Inc., Instant heart rate by azumio, 2015.
[24] Google Inc., Android 4.4 compatibility definition, 2013.
[25] S. Haykin, B. Van Veen, Signals and Systems, John Wiley & Sons, 2002.
[26] L.F. Junqueira Jr., Teaching cardiac autonomic function dynamics employing the valsalva (valsalva-weber) maneuver, Adv. Physiol. Educ. 32 (1) (2008) 100–106.
[27] MathWorks, Inc., Matlab - the language of technical computing, 2015,
[28] Y.C. Chiu, P.W. Arand, S.G. Shroff, T. Feldman, J.D. Carroll, Determination of pulse wave velocities with computerized algorithms., Am. Heart J. 121 (5) (1991) 1460–1470.

Alair Dias Junior is currently the head of the Bachelor Program in Computer Engineering and Professor of Computer Engineering and Computer Science at FUMEC University, Brazil. He received his BS, MS and PhD degrees in Electrical Engineering from the Federal University of Minas Gerais (UFMG), Brazil, in 2005, 2008 and 2012 respectively. His research interests include digital processing of biosignals, and the design and verification of Systems-on-chip (SoCs), embedded systems, and digital integrated circuits in general. Dr. Dias Junior has more than 17 years of experience in industrial automation and embedded systems design and he is the co-founder of the Brazilian start-up Wisecomm. He has also been awarded a Swiss Government Excellence Scholarship to conduct research at the Embedded Systems Laboratory (ESL) of the École Polytechnique Fédérale de Lausanne (EPFL), Switzerland.

Srinivasan Murali is the CEO and co-founder of SmartCardia. He received the MS and PhD degrees in Electrical Engineering from Stanford University in 2007. His research interests include wearable devices and IoT, on-device machine learning and bio-signal analysis and Networks on Chips. He is a recipient of the EDAA outstanding dissertation award for his work on interconnect architecture design. He received a best paper award at the DATE 2005 conference and one of his papers has also been selected as one of The Most Influential Papers of 10 Years DATE. He has authored/co-authored a book, several patents, book chapters and over 50 publications in leading conferences and journals.

Francisco Rincón is a research associate in the Embedded Systems Laboratory (ESL) at École Polytechnique Fédérale de Lausanne (EPFL), Switzerland, and CTO of SmartCardia. He received his MSc and PhD degrees in computer science and engineering from UCM, Spain, in 2006 and 2012, respectively. His current research interests include embedded signal processing and energy-aware optimizations for wearable medical devices. In this field, he is co-author of four U.S. patents.

David Atienza (M'05-SM'13-F'16) is an associate professor of electrical and computer engineering, and director of the Embedded Systems Laboratory (ESL) at École Polytechnique Fédérale de Lausanne (EPFL), Switzerland. He received his MSc and PhD degrees in computer science and engineering from UCM, Spain, and IMEC, Belgium, in 2001 and 2005, respectively. His research interests include system-level design methodologies for high-performance multi-processor system-on-chip (MPSoC) and low-power embedded systems, including new 2-D/3-D thermal-aware design for MPSoCs, ultra-low power system architectures for wireless body sensor nodes, HW/SW reconfigurable systems, dynamic memory optimizations, and network-on-chip design. He is a co-author of more than 200 publications in peer-reviewed international journals and conferences, several book chapters, and five U.S. patents in these fields. He has earned several best paper awards and he is (or has been) an Associate Editor of IEEE TC, IEEE D&T, IEEE T-TCAD, and Elsevier *Integration*. He is the Technical Programme Chair of IEEE/ACM DATE 2015. Dr. Atienza received the IEEE CEDA Early Career Award in 2013, the ACM SIGDA Outstanding New Faculty Award in 2012 and a Faculty Award from Sun Labs at Oracle in 2011. He is a Distinguished Lecturer (period 2014-2015) of the IEEE Circuits and Systems Society (CASS), and an IEEE Fellow and Senior Member of ACM.

Please cite this article as: A. Dias Junior et al., Methods for reliable estimation of pulse transit time and blood pressure variations using smartphone sensors, Microprocessors and Microsystems (2016), http://dx.doi.org/10.1016/j.micpro.2016.06.001